INSTITUT DE FRANCE
Académie des sciences

Comptes Rendus
Mécanique

Thi Thom Tran and Dinh Kien Nguyen

Dynamics of inclined CNTRC sandwich beams under a moving mass with influence of CNT agglomeration

Volume 351 (2023), p. 373-390

Published online: 21 November 2023

https://doi.org/10.5802/crmeca.226

Les Comptes Rendus. Mécanique *sont membres du Centre Mersenne pour l'édition scientifique ouverte*
www.centre-mersenne.org
e-ISSN : 1873-7234

Comptes Rendus
Mécanique
2023, Vol. 351, p. 373-390
https://doi.org/10.5802/crmeca.226

Research article / *Article de recherche*

Dynamics of inclined CNTRC sandwich beams under a moving mass with influence of CNT agglomeration

Dynamique des poutres sandwich CNTRC inclinées sous une masse en mouvement avec influence de l'agglomération des CNT

Thi Thom Tran [a] **and Dinh Kien Nguyen** [*, a, b]

[a] Institute of Mechanics, VAST, 18 Hoang Quoc Viet, Hanoi, Vietnam

[b] VNU, University of Engineering and Technology, 144 Xuan Thuy, Cau Giay, Hanoi, Vietnam

E-mail: ndkien@imech.vast.vn (D. K. Nguyen)

Abstract. Dynamics of inclined carbon nanotube (CNT) reinforced composite beams under a moving mass with influence of CNT agglomeration is studied. The beams compose of a homogeneous core and two composite face layers with effective properties being estimated by Eshelby–Mori–Tanaka approach. A novel finite element formulation is formulated and used to establish the equation of motion. Dynamic response is computed for a simply supported beam by Newmark method. The result reveals the important role of the CNT agglomeration on the dynamic response. The effects of the mass velocity, inclined angle and agglomeration parameters on the dynamic behavior are investigated in detail.

Résumé. La dynamique des poutres composites inclinées renforcées par des nanotubes de carbone (NTC) sous une masse en mouvement avec l'influence de l'agglomération des NTC est étudiée. Les poutres sont composées d'un noyau homogène et de deux couches composites frontales dont les propriétés effectives sont estimées par l'approche Eshelby–Mori–Tanaka. Une nouvelle formulation par éléments finis est formulée et utilisée pour établir l'équation du mouvement. La réponse dynamique est calculée pour une poutre simplement supportée par la méthode de Newmark. Les résultats révèlent le rôle important de l'agglomération des NTC sur la réponse dynamique. Les effets de la vitesse de la masse, de l'angle d'inclinaison et des paramètres d'agglomération sur le comportement dynamique sont étudiés en détail.

Keywords. CNT, Inclined sandwich beam, Moving mass, Trigonometric shear deformation theory, Dynamic analysis.

Mots-clés. NTC, Poutre sandwich inclinée, Masse mobile, Théorie trigonométrique de la déformation par cisaillement, Analyse dynamique.

Funding. Institute of Mechanics, VAST (Vietnam) (Grant agreement no. CSCL03.02/22-23).

Manuscript received 17 May 2023, revised 11 August 2023, accepted 7 September 2023.

* Corresponding author.

1. Introduction

Since the landmark work of Iijimas [1], carbon nanotubes (CNTs) have been considered as an ideal reinforcement component for new generation composites. Thanks to superior mechanical, thermal, thermo-mechanical and vibration characteristics over conventional composites, CNT reinforced structures have drawn great attention from researchers. It has been shown that the mechanical properties of a polymer composite can be considerably enhanced by adding a small amount of CNTs to the matrix. Most studies on mechanical behavior of CNT reinforced composite (CNTRC) structures, however, are considered as aligned single-walled carbon nanotubes (SWCNTs), and the effective material properties are estimated using a very simple method, namely the rule of mixture model (ROM) [2–12].

Due to the high aspect ratio and low bending stiffness, CNTs tend to be agglomerated within the polymer matrix. Rubel *et al.* [13] discussed the effects of CNT agglomerations in composites formation for various CNTs reinforced composites. The authors pointed out that the agglomeration/clustering of CNTs has a direct effect on the thermal, electrical, and mechanical properties of composites and reduces the physical properties. To predict the effective properties such as Young's modulus and Poisson's ratio of composites reinforced by agglomerated CNTs, Shi *et al.* [14] proposed a two-parameter micromechanical model that accounts for the influence of CNT agglomeration. The model in Ref. [14] was used in conjunction with Mori–Tanaka scheme by Heshmati and Yas [15] to derive elastic moduli of randomly oriented CNTRC in a free vibration analysis of functionally graded (FG)-CNTRC beams. Finite element method was adopted in [15] to obtained the beam frequencies. The generalized differential quadrature method (GDQM) was adopted by Nejati and Eslampanah [16] to evaluate natural frequency of a thick cantilever CNTRC beam. The influence of agglomerated CNTs on the natural frequencies of beam reinforced by randomly oriented agglomerated CNTs is considered by the authors. Based on Timoshenko beam theory and the GDQM, Kamarian *et al.* [17] determined free vibration characteristics of FG nanocomposite sandwich beams on Pasternak foundation, considering the agglomeration effect of SWCNTs. The GDQM was also employed in [18] to study vibration of non-uniform agglomerated CNTRC beams with piezoelectric layers. A two-parameter model based on a combination of self-consistent and Mori–Tanaka method was presented by Pan and Bian [19] for investigating the effect of aggregation on CNT reinforced composites. It was concluded by the authors that the CNT agglomeration reduces the elastic stiffness of composites, while the uniformly dispersed CNTs enhance the reinforcement. Kiani *et al.* [20] presented a thermo-mechanical buckling analysis of CNTRC beams under non-uniform thermal loading, also considering the CNT agglomeration. Hamilton's principle was adopted to construct the governing equations, and the GDQM was used to obtain the solution. Yue *et al.* [21] introduced a quasi-3D beam model in their investigation of the effect of CNT agglomeration on the nonlinear dynamic stability of CNTRC beams.

The problem of inclined beams under the moving loads is practically important, and it draws much attention from researchers. As positions of the dynamic loads vary with time, special techniques are required to analyze this problem. In an early work, the finite element method was used by Wu [22] to study dynamics of an inclined isotropic Euler–Bernoulli beam subjected to a moving mass. The influence of the inertia, Coriolis and centrifugal forces was taken into consideration in the study. The author concluded that the transverse displacement of the beam decreases considerably by increasing the inclined angle. Also using the finite element method and Euler–Bernoulli beam theory, Bahmyari *et al.* [23] investigated dynamic response of laminated composite beams under moving distributed masses. It has been shown that the deflection of the inclined beams is remarkably influenced by the friction force, while it is not considerably affected by the Coriolis and centrifugal forces. An equivalent horizontal beam model in which the force acting on the inclined beam is split into the transverse and axial forces, is

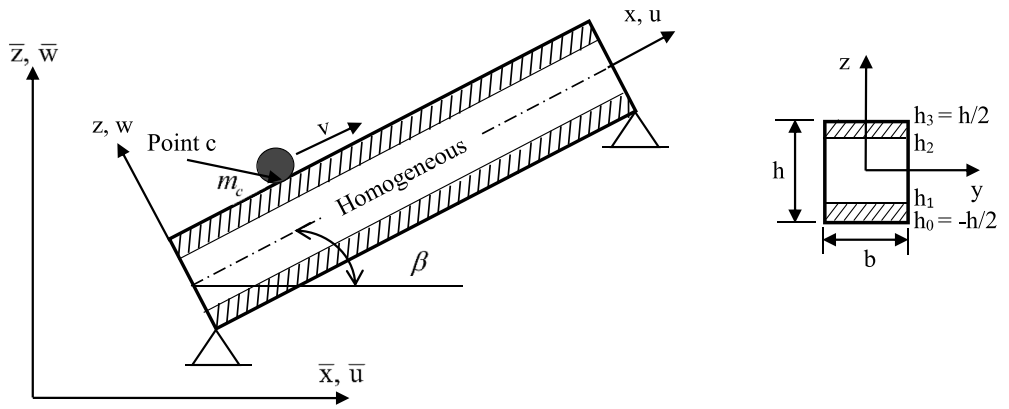

Figure 1. A simply supported inclined CNTRC sandwich beam under a moving mass.

proposed by Mamandi *et al.* [24] for the geometrically nonlinear dynamic analysis of an inclined Euler–Bernoulli beam under a moving force. The work was then extended by Mamandi and Kargarnovin [25] to investigate the nonlinear dynamic response of Timoshenko beams subjected to moving masses. The numerical results in Refs. [24, 25] show that the geometric nonlinearity stiffens the dynamic response of the beams. Recently, Nguyen *et al.* [26] presented a third-order shear deformation theory based finite element procedure for dynamic analysis of an inclined functionally graded sandwich beam carrying a moving mass. The material properties of the beam are considered to vary in both the axial and the transverse directions by the power gradation laws.

As seen from the above literature review, the dynamic analysis of inclined beams under moving loads has not been considered sufficiently. Motivated by this fact, this paper studies dynamics of inclined CNTRC sandwich beams under a moving mass, taking into account the influence of CNTs agglomeration. The sandwich beams are composed of a homogeneous core and two face sheets made from CNTRC material. The effective properties of the composite face sheets are estimated by Eshelby–Mori–Tanaka approach. Based on the trigonometric shear deformation theory, a novel finite element formulation, taking into account the influence of the inertial, Coriolis and centrifugal forces, is derived and used to establish the discretized equation of motion for the beams. To improve efficiency of the formulation, the transverse shear rotation instead of the conventional section rotation is employed herein as an independent variable. The effects of various parameters, including the CNT volume fraction, the agglomeration parameters, the layer thickness ratio, the mass velocity as well as the inclined angle on the dynamic behavior of the sandwich beams are investigated in detail and highlighted.

2. Inclined sandwich beam reinforced with agglomerated CNTs

Figure 1 shows an inclined sandwich beam under a moving mass m_c in two Cartesian coordinate systems, a local system (x, z) and a global one $(\overline{x}, \overline{z})$. The sandwich beam has three layers, a homogeneous core and two face layers made of CNT reinforced composite. The x-axis of the (x, z) system is chosen on the beam's mid-plane. The mass m_c is assumed to move with a constant velocity v, and it is always in contact with the beam. Denoted in Figure 1, L, b, h, h_0, h_1, h_2, h_3 and β are, respectively, the length, width and height of the beam, the vertical coordinates of bottom surface, the interfaces between the layers, the top surface and the inclined angle.

The two-parameter micromechanical model of Shi *et al.* [14] is adopted herein to account for the CNT agglomeration. The model is developed by considering a representative volume element

(RVE) with Eshelby cluster model of CNT agglomeration, as depicted in Figure 2. The total volume V_r of CNTs in the RVE is divided into two parts as:

$$V_r = V_r^{\text{cluster}} + V_r^m \tag{1}$$

where V_r^{cluster} and V_r^m are the volumes of CNTs inside and outside of the cluster, respectively. The CNT agglomeration is described by two following parameters:

$$\xi = \frac{V_{\text{cluster}}}{V}, \quad \zeta = \frac{V_r^{\text{cluster}}}{V_r}, \quad 0 \le \xi, \zeta \le 1 \tag{2}$$

where V_{cluster} denotes the volume of clusters in the RVE. Thus, the parameter ξ in Equation (2) is the volume fraction of clusters with respect to the RVE volume, the parameter ζ is the ratio of CNT volume inside the clusters over the total volume of the CNTs inside the RVE. The case, $\xi = 1$ means that CNTs are uniformity distributed in the matrix; a lower value of ξ is the more agglomeration of CNTs. When $\zeta = 1$, all CNTs are located inside the clusters. The case $\xi = \zeta$ means that the volume fraction of CNTs inside the clusters is the same as that of CNTs outside the clusters. In the case $\zeta > \xi$, the value of ζ is bigger, the distribution of CNTs is more heterogeneous. The effective bulk and shear moduli of the clusters $K_{\text{in}}, G_{\text{in}}$, and those of the region outside the clusters $K_{\text{out}}, G_{\text{out}}$ may be calculated by [14]:

$$\begin{aligned}
K_{\text{in}} &= K_m + \frac{V_{\text{CNT}}\zeta(\delta_r - 3K_m\alpha_r)}{3(\xi - V_{\text{CNT}}\zeta + V_{\text{CNT}}\zeta\alpha_r)},\\
G_{\text{in}} &= G_m + \frac{V_{\text{CNT}}\zeta(\eta_r - 2G_m\beta_r)}{2(\xi - V_{\text{CNT}}\zeta + V_{\text{CNT}}\zeta\beta_r)},\\
K_{\text{out}} &= K_m + \frac{V_{\text{CNT}}(1-\zeta)(\delta_r - 3K_m\alpha_r)}{3[1-\xi - V_{\text{CNT}}(1-\zeta) + V_{\text{CNT}}(1-\zeta)\alpha_r]},\\
G_{\text{out}} &= G_m + \frac{V_{\text{CNT}}(1-\zeta)(\eta_r - 2G_m\beta_r)}{2[1-\xi - V_{\text{CNT}}(1-\zeta) + V_{\text{CNT}}(1-\zeta)\zeta\beta_r]}
\end{aligned} \tag{3}$$

with $V_{\text{CNT}} = V_r/V$ is CNT volume fraction in the composite, and

$$\begin{aligned}
\alpha_r &= \frac{3(K_m + G_m) + k_r - l_r}{3(G_m + k_r)},\\
\delta_r &= \frac{1}{3}\left[n_r + 2l_r + \frac{(2k_r + l_r)(3K_m + 2G_m - l_r)}{G_m + k_r}\right],\\
\beta_r &= \frac{1}{5}\left(\frac{4G_m + 2k_r + l_r}{3(G_m + k_r)} + \frac{4G_m}{G_m + p_r} + \frac{2[G_m(3K_m + G_m) + G_m(3K_m + 7G_m)]}{G_m(3K_m + G_m) + m_r(3K_m + 7G_m)}\right),\\
\eta_r &= \frac{1}{5}\left[\frac{2}{3}(n_r - l_r) + \frac{8G_m p_r}{G_m + p_r} + \frac{8m_r G_m(3K_m + 4G_m)}{3K_m(m_r + G_m) + G_m(7m_r + G_m)} + \frac{(2k_r - l_r)(2G_m + l_r)}{3(G_m + k_r)}\right]
\end{aligned} \tag{4}$$

with $K_m = E_m/3(1-2\upsilon_m)$, $G_m = E_m/2(1+\upsilon_m)$ are the bulk and shear moduli of the matrix, respectively. In Equations (3) and (4), the subscripts m and r stand for the quantities of the matrix and the reinforcing phase (CNTs); k_r, l_r, m_r, n_r, p_r are the Hill's elastic moduli for the reinforcing phase.

The effective bulk modulus K and shear modulus G of the composite evaluated by the Mori–Tanaka scheme, scheme that satisfies Hanshin–Shtrikman bounds [27], are of the forms [14]:

$$K = K_{\text{out}}\left(1 + \frac{\xi\left(\frac{K_{\text{in}}}{K_{\text{out}}} - 1\right)}{1 + \alpha(1-\xi)\left(\frac{K_{\text{in}}}{K_{\text{out}}} - 1\right)}\right), \quad G = G_{\text{out}}\left(1 + \frac{\xi\left(\frac{G_{\text{in}}}{G_{\text{out}}} - 1\right)}{1 + \beta(1-\xi)\left(\frac{G_{\text{in}}}{G_{\text{out}}} - 1\right)}\right) \tag{5}$$

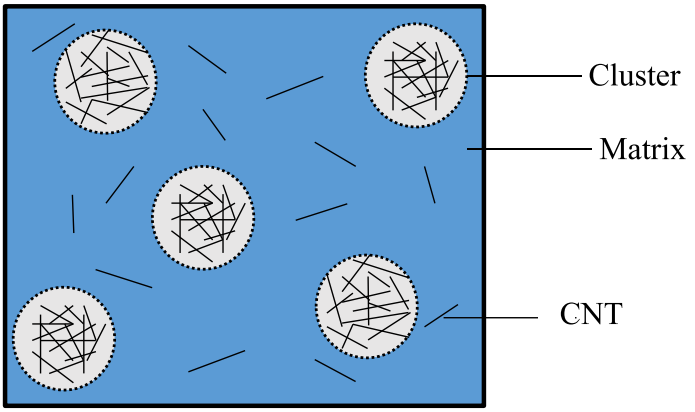

Figure 2. RVE with Eshelby cluster model of agglomeration of CNTs.

where $\alpha = (1+\nu_{\text{out}})/3(1-\nu_{\text{out}})$, $\beta = (8-10\nu_{\text{out}})/15(1-\nu_{\text{out}})$, $\nu_{\text{out}} = (3K_{\text{out}}-2G_{\text{out}})/2(3K_{\text{out}}+G_{\text{out}})$. Noting that the composite is considered to be isotropic for the case CNTs are oriented completely at random throughout the matrix. In this case, the bulk and shear moduli have the following forms [14]:

$$K = K_m + \frac{V_{\text{CNT}}(\delta_r - 3K_m\alpha_r)}{3(c_m + V_{\text{CNT}}\alpha_r)}, \quad G = G_m + \frac{V_{\text{CNT}}(\eta_r - 2G_m\beta_r)}{2(c_m + V_{\text{CNT}}\beta_r)} \tag{6}$$

where $c_m = 1 - V_{\text{CNT}}$, and α_r, δ_r, β_r, η_r are given in Equation (4). The effective Young's modulus E and the Poisson's ratio ν of the CNT reinforced layer can be derived by:

$$E = \frac{9KG}{3K+G}; \quad \nu = \frac{3K-2G}{6K+2G}. \tag{7}$$

Meanwhile, the effective mass density of the CNT reinforced layer can be estimated by the rule of mixture as [28]:

$$\rho = (\rho^{\text{CNT}} - \rho^m)V_{\text{CNT}} + \rho^m \tag{8}$$

with ρ^{CNT}, ρ^m are the mass density of CNT and matrix, respectively.

3. Mathematical formulation

Based on the trigonometric shear deformation theory [29], the displacements in x and z directions of a point in the sandwich are given as:

$$u(x,z,t) = u_0(x,t) - zw_{0,x} + \sin\frac{\pi z}{h}\theta; \quad w(x,z,t) = w_0(x,t) \tag{9}$$

where $u_0(x,t)$, $w_0(x,t)$ are the displacements of a point on the x axis; θ is the cross-sectional rotation, and t is the time variable. In Equation (9) and hereafter, the subscript comma indicates the derivative with respect to the variable that followed.

In order to improve the finite element formulation derived in the next section, the transverse shear rotation $\gamma_0 = \theta + w_{0,x}$, not the conventional cross-sectional rotation θ, is employed herein as the independent variable instead. In this regard, the displacements in Equation (9) can be rewritten in the form:

$$u(x,z,t) = u_0(x,t) - zw_{0,x} + \sin\frac{\pi z}{h}(\gamma_0 - w_{0,x}); \quad w(x,z,t) = w_0(x,t). \tag{10}$$

The strain field associated with the displacement field in Equation (10) is of the form:

$$\varepsilon_{xx} = u_{0,x} - zw_{0,xx} + \sin\frac{\pi z}{h}(\gamma_{0,x} - w_{0,xx}); \quad \gamma_{xz} = \frac{\pi}{h}\cos\frac{\pi z}{h}(\gamma_0 - w_{0,x}) \tag{11}$$

where ε_{xx} and γ_{xz} are axial and shear strains, respectively.

The stress–strain relations in the kth layer with the Hook's law assumption are as follows:

$$\sigma_{xx}^{(k)} = E^{(k)}\varepsilon_{xx}; \quad \tau_{xz}^{(k)} = G^{(k)}\gamma_{xz} \quad (k = 1,2,3). \tag{12}$$

One can verify that the adopted theory satisfies the free transverse shear stress conditions on the top and bottom surfaces of the beam. The elastic strain energy of the sandwich beam U is given by:

$$\begin{aligned} U &= \frac{1}{2}\int_0^L \int_A (\sigma_{xx}^{(k)}\varepsilon_{xx} + \tau_{xz}^{(k)}\gamma_{xz})\,\mathrm{d}A\,\mathrm{d}x \\ &= \frac{1}{2}\int_0^L \left[\begin{matrix} A_1 u_{0,x}^2 - 2A_2 u_{0,x} w_{0,xx} + 2A_3 u_{0,x}(\gamma_{0,x} - w_{0,xx}) - 2A_4 w_{0,xx}(\gamma_{0,x} - w_{0,xx}) \\ +A_5(\gamma_{0,x} - w_{0,xx})^2 + A_6 w_{0,xx}^2 + A_7(\gamma_0 - w_{0,x})^2 \end{matrix}\right] \mathrm{d}x \end{aligned} \tag{13}$$

where $A = bh$ is the area of cross section of the beam; $A_1, A_2, \ldots, A_7$ are the beam rigidities, defined as follows:

$$\begin{aligned} (A_1, A_2, A_3, A_4, A_5, A_6) &= b\int_{h_0}^{h_3} E\left(1, z, \sin\frac{\pi z}{h}, z\sin\frac{\pi z}{h}, \sin^2\frac{\pi z}{h}, z^2\right)\mathrm{d}z \\ &= b\sum_{k=1}^{3}\int_{h_{k-1}}^{h_k} E^{(k)}\left(1, z, \sin\frac{\pi z}{h}, z\sin\frac{\pi z}{h}, \sin^2\frac{\pi z}{h}, z^2\right)\mathrm{d}z; \end{aligned} \tag{14}$$

$$A_7 = b\frac{\pi^2}{h^2}\int_{h_0}^{h_3} G\cos^2\frac{\pi z}{h}\,\mathrm{d}z = b\frac{\pi^2}{h^2}\sum_{k=1}^{3}\int_{h_{k-1}}^{h_k} G^{(k)}\cos^2\frac{\pi z}{h}\,\mathrm{d}z.$$

The kinetic energy T of the sandwich beam can be expressed as:

$$\begin{aligned} T &= \frac{1}{2}\int_0^L \int_A \rho(\dot{u}^2 + \dot{w}^2)\,\mathrm{d}A\,\mathrm{d}x \\ &= \frac{1}{2}\int_0^L \left[\begin{matrix} I_1(\dot{u}_0^2 + \dot{w}_0^2) - 2I_2\dot{u}_0\dot{w}_{0,x} + 2I_3\dot{u}_0(\dot{\gamma}_0 - \dot{w}_{0,x}) \\ -2I_4\dot{w}_{0,x}(\dot{\gamma}_0 - \dot{w}_{0,x}) + I_5(\dot{\gamma}_0 - \dot{w}_{0,x})^2 + I_6\dot{w}_{0,x}^2 \end{matrix}\right]\mathrm{d}x. \end{aligned} \tag{15}$$

The over dot in Equation (15), and hereafter, denotes the derivative with respect to time variable t; $I_1, I_2, \ldots, I_6$ are mass moments, defined as:

$$\begin{aligned} (I_1, I_2, I_3, I_4, I_5, I_6) &= b\int_{h_0}^{h_3} \rho\left(1, z, \sin\frac{\pi z}{h}, z\sin\frac{\pi z}{h}, \sin^2\frac{\pi z}{h}, z^2\right)\mathrm{d}z \\ &= b\sum_{k=1}^{3}\int_{h_{k-1}}^{h_k} \rho^{(k)}\left(1, z, \sin\frac{\pi z}{h}, z\sin\frac{\pi z}{h}, \sin^2\frac{\pi z}{h}, z^2\right)\mathrm{d}z. \end{aligned} \tag{16}$$

When the beam is inclined an angle β and subjected to the moving mass m_c, the potential energy is calculated as follows [25]:

$$V = \int_0^L [(-m_c g\cos\beta + m_c\ddot{w}_0 + 2m_c v\dot{w}_{0,x} + m_c v^2 w_{0,xx})w_0 + (-m_c g\sin\beta + m_c\ddot{u}_0)u_0]\delta(x - vt)\,\mathrm{d}x \tag{17}$$

where $P_x = -m_c g\sin\beta$, $P_z = -m_c g\cos\beta$ are force components induced by the mass m_c with $g = 9.81\ \mathrm{m/s^2}$ is the acceleration of gravity; $m_c\ddot{u}_0$ and $m_c\ddot{w}_0$ are components of the inertial force; $2m_c v\dot{w}_{0,x}$ is the Coriolis force and $m_c v^2 w_{0,xx}$ is centrifugal force; $\delta(.)$ is the Dirac delta function; x is the abscissa of the moving mass, respect to the left end of the beam. One can obtain the differential equations of motion for the beam by applying Hamilton's principle to Equations (13), (15) and (17). However, due to the material heterogeneity as well as the non-traditional inclined beam configuration, a closed-form solution for such equations is hardly obtained. Finite element formulation derived in the next section is a reasonable choice to compute the dynamic response of the beam.

4. Finite element formulation

A two-node beam element, (1, 2), with length l is firstly derived in the local system (x, z) and then transferred to the global one in this work. Each node of the element has four degrees of freedom, namely the axial displacement, transverse displacement, derivative of the transverse displacement and the shear rotation. Thus, the element vector of nodal displacements ($\mathbf{d}$) has the form:

$$\mathbf{d} = \{\mathbf{d}_u \ \mathbf{d}_w \ \mathbf{d}_\gamma\}^T \tag{18}$$

where

$$\mathbf{d}_u = \{u_{01}\, u_{02}\}^T; \quad \mathbf{d}_w = \{w_{01}\, w_{0x1}\, w_{02}\, w_{0x2}\}^T; \quad \mathbf{d}_\gamma = \{\gamma_{01}\gamma_{02}\}^T \tag{19}$$

are, respectively, the vectors of nodal displacement for u_0, w_0 and γ_0 at the nodes 1 and 2. In the above equations and hereafter, a superscript "T" denotes the transpose of a vector or a matrix.

The displacements and shear rotation inside the element are interpolated through their nodal values according to:

$$u_0 = \mathbf{N}\mathbf{d}_u; \quad w_0 = \mathbf{H}\mathbf{d}_w; \quad \gamma_0 = \mathbf{N}\mathbf{d}_\gamma \tag{20}$$

where $\mathbf{N} = \{N_1 N_2\}$ is the matrix of the following linear interpolation functions

$$N_1 = 1 - \frac{x}{l},\ N_2 = \frac{x}{l} \tag{21}$$

and $\mathbf{H} = \{H_1 \ H_2 \ H_3 \ H_4\}$ is the matrix of Hermite shape functions with

$$H_1 = 1 - 3\left(\frac{x}{l}\right)^2 + 2\left(\frac{x}{l}\right)^3, \quad H_2 = x - 2\frac{x^2}{l} + \frac{x^3}{l^2}, \quad H_3 = 3\left(\frac{x}{l}\right)^2 - 2\left(\frac{x}{l}\right)^3, \quad H_4 = -\frac{x^2}{l} + \frac{x^3}{l^2}. \tag{22}$$

Using the interpolations, one can write the strain energy in Equation (13) in the form:

$$U = \frac{1}{2}\sum_{i=1}^{ne} \mathbf{d}_i^T \mathbf{k}_i \mathbf{d}_i \tag{23}$$

where ne is the total number of elements used to discretize the sandwich beam, and $\mathbf{k}$ is the element stiffness matrix with the following form:

$$\mathbf{k} = \begin{bmatrix} \mathbf{k}_{u_0u_0} & \mathbf{k}_{u_0w_0} & \mathbf{k}_{u_0\gamma_0} \\ \mathbf{k}_{u_0w_0}^T & \mathbf{k}_{w_0w_0} & \mathbf{k}_{w_0\gamma_0} \\ \mathbf{k}_{u_0\gamma_0}^T & \mathbf{k}_{w_0\gamma_0}^T & \mathbf{k}_{\gamma_0\gamma_0} \end{bmatrix}. \tag{24}$$

In Equation (24), $\mathbf{k}_{u_0u_0}, \mathbf{k}_{u_0w_0}, \ldots, \mathbf{k}_{\gamma_0\gamma_0}$ are, respectively, the element stiffness matrices stemming from the axial, bending, shear deformations and their couplings with the following expressions:

$$\begin{aligned}
\mathbf{k}_{u_0u_0} &= \int_0^l \mathbf{N}_{,x}^T A_1 \mathbf{N}_{,x}\, \mathrm{d}x, \quad \mathbf{k}_{w_0w_0} = \int_0^l [\mathbf{H}_{,xx}^T (2A_4 + A_5 + A_6)\mathbf{H}_{,xx} + \mathbf{H}_{,x}^T A_7 \mathbf{H}_{,x}]\, \mathrm{d}x, \\
\mathbf{k}_{\gamma_0\gamma_0} &= \int_0^l (\mathbf{N}_{,x}^T A_5 \mathbf{N}_{,x} + \mathbf{N}^T A_7 \mathbf{N})\, \mathrm{d}x, \\
\mathbf{k}_{u_0w_0} &= -\int_0^l \mathbf{N}_{,x}^T (A_2 + A_3)\mathbf{H}_{,xx}\, \mathrm{d}x, \quad \mathbf{k}_{u_0\gamma_0} = \int_0^l \mathbf{N}_{,x}^T A_3 \mathbf{N}_{,x}\, \mathrm{d}x, \\
\mathbf{k}_{w_0\gamma_0} &= -\int_0^l [\mathbf{H}_{,xx}^T (A_4 + A_5)\mathbf{N}_{,x} + \mathbf{H}_{,x}^T A_7 \mathbf{N}]\, \mathrm{d}x.
\end{aligned} \tag{25}$$

Similarly, the kinetic energy of the beam in Equation (15) can be rewritten as

$$T = \frac{1}{2}\sum_{i=1}^{ne} \dot{\mathbf{d}}_i^T \mathbf{m}_i \dot{\mathbf{d}}_i \tag{26}$$

where the element mass matrix of the beam $\mathbf{m}$ can be written in sub-matrices as

$$\mathbf{m} = \begin{bmatrix} \mathbf{m}_{u_0u_0} & \mathbf{m}_{u_0w_0} & \mathbf{m}_{u_0\gamma_0} \\ \mathbf{m}_{u_0w_0}^T & \mathbf{m}_{w_0w_0} & \mathbf{m}_{w_0\gamma_0} \\ \mathbf{m}_{u_0\gamma_0}^T & \mathbf{m}_{w_0\gamma_0}^T & \mathbf{m}_{\gamma_0\gamma_0} \end{bmatrix} \tag{27}$$

in which

$$\begin{aligned} \mathbf{m}_{u_0u_0} &= \int_0^l \mathbf{N}^T A_1 \mathbf{N}\,\mathrm{d}x, \quad \mathbf{m}_{w_0w_0} = \int_0^l [\mathbf{H}_{,x}^T (2I_4 + I_5 + I_6)\mathbf{H}_{,x} + \mathbf{H}^T I_1 \mathbf{H}]\,\mathrm{d}x, \\ \mathbf{m}_{\gamma_0\gamma_0} &= \int_0^l (\mathbf{N}^T I_5 \mathbf{N})\,\mathrm{d}x, \quad \mathbf{m}_{u_0w_0} = -\int_0^l \mathbf{N}^T (I_2 + I_3)\mathbf{H}_{,x}\,\mathrm{d}x, \\ \mathbf{m}_{u_0\gamma_0} &= \int_0^l \mathbf{N}^T I_3 \mathbf{N}\,\mathrm{d}x, \quad \mathbf{m}_{w_0\gamma_0} = -\int_0^l \mathbf{H}_{,xx}^T (I_4 + I_5)\mathbf{N}_{,x}\,\mathrm{d}x. \end{aligned} \tag{28}$$

The potential energy in Equation (17) is now of the form:

$$V = \sum^{ne} (\ddot{\mathbf{d}}^T \mathbf{m}_m \ddot{\mathbf{d}} + \dot{\mathbf{d}}^T \mathbf{c}_m \dot{\mathbf{d}} + \mathbf{d}^T \mathbf{k}_m \mathbf{d} - \mathbf{d}^T \mathbf{f}_m), \tag{29}$$

where $\mathbf{m}_m$, $\mathbf{c}_m$ and $\mathbf{k}_m$ are, respectively, the element mass, damping and stiffness matrices due to the effects of the inertia, Coriolis and centrifugal forces of the moving mass; $\mathbf{f}_m$ is the time-dependent element nodal load vector generated by the moving mass. The expressions for these matrices and vector are as follows:

$$\underset{8\times8}{\mathbf{m}_m} = m_c \begin{bmatrix} \mathbf{N}^T\mathbf{N} & \mathbf{0} & \mathbf{0} \\ \mathbf{0} & \mathbf{H}^T\mathbf{H} & \mathbf{0} \\ \mathbf{0} & \mathbf{0} & \mathbf{0} \end{bmatrix}_{|x_c}, \quad \underset{8\times8}{\mathbf{c}_m} = 2m_c v \begin{bmatrix} \mathbf{0} & \mathbf{0} & \mathbf{0} \\ \mathbf{0} & \mathbf{H}^T\mathbf{H}_{,x} & \mathbf{0} \\ \mathbf{0} & \mathbf{0} & \mathbf{0} \end{bmatrix}_{|x_c}, \quad \underset{8\times8}{\mathbf{k}_m} = m_c v^2 \begin{bmatrix} \mathbf{0} & \mathbf{0} & \mathbf{0} \\ \mathbf{0} & \mathbf{H}^T\mathbf{H}_{,xx} & \mathbf{0} \\ \mathbf{0} & \mathbf{0} & \mathbf{0} \end{bmatrix}_{|x_c}, \tag{30}$$

$$\underset{8\times1}{\mathbf{f}_m} = \{P_x\mathbf{N}^T \; P_z\mathbf{H}^T \; \mathbf{0}\}_{|x_c}^T. \tag{31}$$

In Equations (30) and (31), the notation $(.)_{|x_c}$ means that the expression (.) is evaluated at x_c—the current abscissa of the moving mass with respect to the element left node.

The above element matrices and vector are derived in the local coordinate system and they are necessarily transferred to the global system. To this end, we considered the displacements of a point in the beam with respect to the global $\overline{x}$ and $\overline{z}$ directions, $\overline{u}$ and $\overline{w}$. These displacements are related to the ones in the local x and z directions, u and w by:

$$\overline{u} = u\cos\beta - w\sin\beta; \quad \overline{w} = u\sin\beta + w\cos\beta. \tag{32}$$

Because the local rotation and the global one are identical, the vector of local degrees of freedom ($\mathbf{d}$) is related to the global one $\overline{\mathbf{d}} = \{\overline{\mathbf{d}}_u \; \overline{\mathbf{d}}_w \; \overline{\mathbf{d}}_\gamma\}^T$ by $\mathbf{d} = \mathbf{T}\overline{\mathbf{d}}$ where the transformation matrix $\mathbf{T}$ having the form:

$$\mathbf{T} = \begin{bmatrix} \cos\beta & 0 & \sin\beta & 0 & 0 & 0 & 0 & 0 \\ 0 & \cos\beta & 0 & 0 & \sin\beta & 0 & 0 & 0 \\ -\sin\beta & 0 & \cos\beta & 0 & 0 & 0 & 0 & 0 \\ 0 & 0 & 0 & 1 & 0 & 0 & 0 & 0 \\ 0 & -\sin\beta & 0 & 0 & \cos\beta & 0 & 0 & 0 \\ 0 & 0 & 0 & 0 & 0 & 1 & 0 & 0 \\ 0 & 0 & 0 & 0 & 0 & 0 & 1 & 0 \\ 0 & 0 & 0 & 0 & 0 & 0 & 0 & 1 \end{bmatrix}. \tag{33}$$

The global element stiffness and mass matrices are finally computed as:

$$\overline{\mathbf{k}} = \mathbf{T}^T\mathbf{k}\mathbf{T}, \quad \text{and} \quad \overline{\mathbf{m}} = \mathbf{T}^T\mathbf{m}\mathbf{T}. \tag{34}$$

Table 1. Hill's elastic modulus for the CNTs [28]

CNT radius (Å)	k_r (GPa)	l_r (GPa)	m_r (GPa)	n_r (GPa)	p_r (GPa)
10	30	10	1	450	1

Similarly, the element mass, damping, stiffness matrices and nodal load vector in Equations (30) and (31) written in global coordinate system are as follows:

$$\overline{\mathbf{m}}_m = \mathbf{T}^T\mathbf{m}_m\mathbf{T}; \quad \overline{\mathbf{c}}_m = \mathbf{T}^T\mathbf{c}_m\mathbf{T}; \quad \overline{\mathbf{k}}_m = \mathbf{T}^T\mathbf{k}_m\mathbf{T}; \quad \overline{\mathbf{f}}_m = \mathbf{T}^T\mathbf{f}_m. \tag{35}$$

The equation for the dynamic analysis of the inclined sandwich beam can now be written as:

$$\overline{\mathbf{M}}\,\ddot{\overline{\mathbf{D}}} + \overline{\mathbf{C}}\,\dot{\overline{\mathbf{D}}} + \overline{\mathbf{K}}\,\overline{\mathbf{D}} = \overline{\mathbf{F}}^{\text{ex}} \tag{36}$$

where $\overline{\mathbf{M}}$, $\overline{\mathbf{K}}$ are the instantaneous overall mass and stiffness matrices, respectively. These matrices composed of the constant overall mass and stiffness matrices of the inclined beam itself and the time-dependent element property matrices due to the moving mass. The overall damping matrix $\overline{\mathbf{C}}$ is obtained by adding the element damping matrix $\overline{\mathbf{c}}_m$ to the damping matrix of the inclined beam itself. The overall damping matrix of the inclined beam is proportional to the overall mass and stiffness matrices by using the theory of Rayleigh damping with a damping ratio of 5%.

5. Numerical results and discussion

This section presents the numerical results on dynamic response of the inclined sandwich beam subjected to the moving mass. Otherwise stated, a sandwich beam with $L/h = 20$, $b = 0.4$ m, $h = 1$ m is considered. The beam is simply supported at both ends, and the geometric boundary conditions are as follows:

$$\text{At } x = 0\text{: } \overline{u}_0(0,t) = \overline{w}_0(0,t) = 0,$$
$$\text{At } x = L\text{: } \overline{u}_0(L,t) = \overline{w}_0(L,t) = 0$$

with $\overline{u}_0$ and $\overline{w}_0$ are the displacements in $\overline{x}$ and $\overline{z}$ directions of a point on the x-axis, respectively. The beam is asumed initially at rest, and all the displacements and velocities at time $t = 0$ equal to zero.

The material properties of the matrix are $E_m = 10$ GPa, $\rho_m = 1150$ kg/m^3, $\nu_m = 0.3$. The armchair (10, 10) SWCNTs with $\rho^{\text{CNT}} = 1400$ kg/m^3 and elastic constants tabulated in Table 1 are used as the reinforcements. The core of the sandwich beam is assumed pure matrix material.

Three numbers in parentheses, e.g. (2-1-1), are used below to denote the layer thickness ratio of the beam layers, from the bottom layer to the top layer. A moving mass $m_c = 0.5\rho_m AL$ is employed in all computations reported below. To facilitate the discussion, the dimensionless parameter is introduced for dynamic magnification factor (DMF) D_d as follows:

$$D_d = \max\left(\frac{w_0(L/2,t)}{w_{st}}\right), \tag{37}$$

where $w_{st} = L^3 m_c g/48E_m I$ is the static deflection of a horizontal beam made of fully core material under mid-span concentrated load $P = m_c g$, and I is the inertia moment of area of the cross-section. A uniform increment time step $\Delta t = \Delta T/200$ with ΔT is the total time needed for the mass crossing the beam, is used for the Newmark procedure.

5.1. *Formulation verification*

In order to examine the accuracy and reliability of the present formulation, the effective Young's modulus and Poisson's ratio of an agglomerated randomly oriented CNTRC beam obtained in the present work are firstly compared with that of Daghigh *et al.* [28] in Figures 3 and 4, respectively.

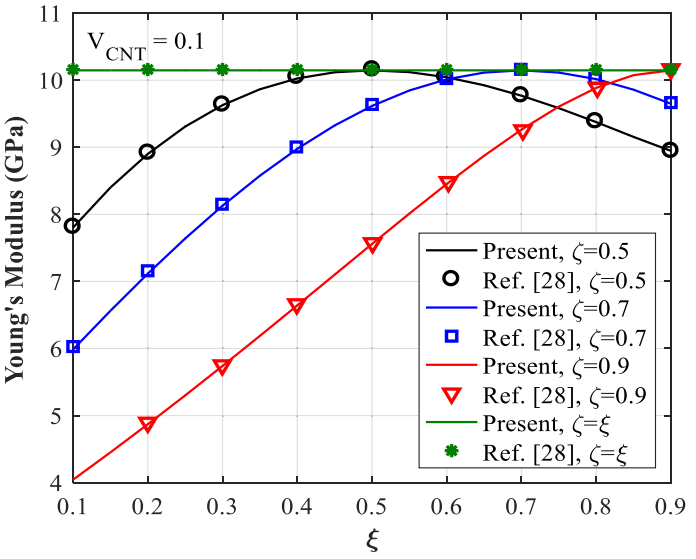

Figure 3. Comparison of effective Young's modulus of CNTRC for $V_{\text{CNT}} = 0.1$ and different agglomeration parameters.

The result in the figures is obtained for a matrix phase with $E_m = 2.5$ GPa, the Hill's elastic moduli for the CNTs listed in Table 1 and CNT volume fraction $V_{\text{CNT}} = 0.1$. A good agreement between the results of the present work with that of Ref. [28] is seen from the figures. The figures show the significant influence of the agglomeration parameters on the effective elastic coefficients of the CNTRC material. Specifically, the effective Young's modulus increases with the increase of ξ, and it approaches the largest value at $\xi = \zeta$, corresponding to the full dispersion of CNTs. On the contrary, the effective Poisson's ratio decreases by increasing the parameter ξ, and then reaches the smallest when $\xi = \zeta$.

In Figure 5, the time histories for mid-span deflection of an inclined homogeneous beam under a moving mass obtained by present formulation are compared with that of Mamandi and Kargarnovin [25] for $\beta = \pi/5$ and various values of the mass velocity parameter, namely $\alpha = 0.1$, 0.25 and 0.5. The velocity parameter α is defined as $\alpha = v/v_{cr}$, with $v_{cr} = (\pi/L)\sqrt{EI/\rho A}$ is the critical velocity of a moving force on a simply supported beam. Good agreement between the time histories of the present work with that of Ref. [25] is noted from Figure 5.

Convergence of the derived formulation in evaluating the fundamental frequency parameter $\lambda^2 = \omega L^2\sqrt{\rho_m A/E_m I}$ ($I = bh^3/12$) of a CNTRC beam is shown in Table 2 for $V_{\text{CNT}} = 0.075$ and two types of boundary conditions, namely fixed at one end and free at the other (CF), and simply supported at both ends (SS). For the sake of comparison, the result obtained by 100 Timoshenko beam elements of Yas and Heshmati [30] is also given in the table. The table shows the fast convergence of the present formulation, and it needs only 14 and 18 elements for the CF and SS beams to converge, respectively. The difference between the frequency parameters of the present work with that of Ref. [30] may be resulted from the different beam theories employed in the two works, and more important is that the effect of CNT agglomeration is not considered in [30].

Table 3 shows the convergence of the present formulation in computing the dynamic magnification factor of the (2-1-2) and (2-2-1) sandwich beams for $\beta = \pi/5$, $V_{\text{CNT}} = 0.1$, $\zeta = 1$ and $v = 20$ m/s. As can be seen from the table, for all considered cases the convergence is achieved by using 28 elements. In this regards, a mesh of 28 elements is employed in all computations reported below.

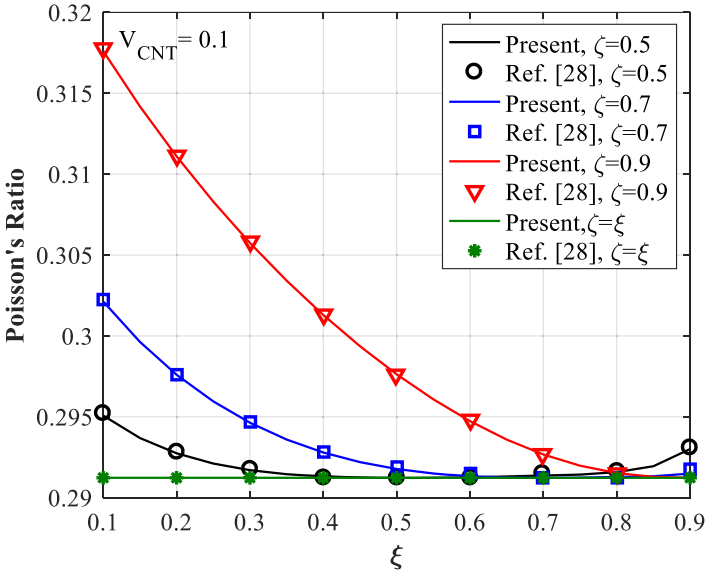

Figure 4. Comparison of Poisson's ratio of CNTRC for $V_{\mathrm{CNT}} = 0.1$ and different agglomeration parameters.

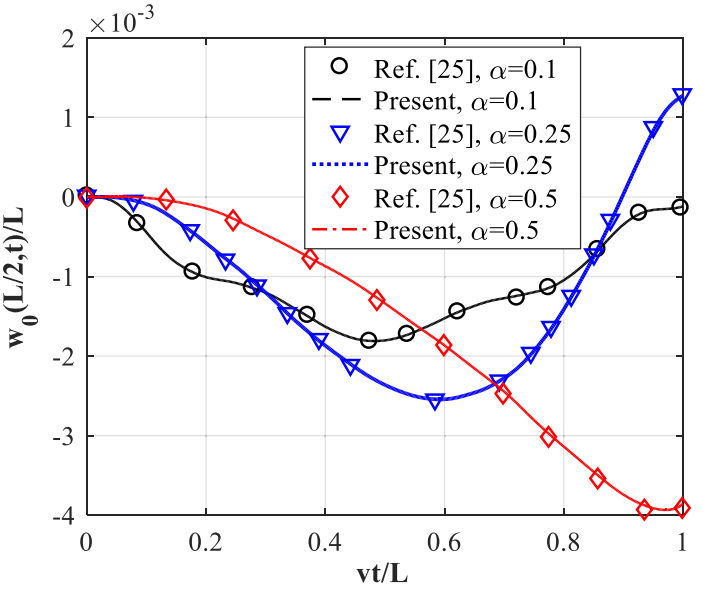

Figure 5. Comparison of time histories for mid-span deflection of inclined homogeneous beam with $\beta = \pi/5$.

5.2. *Dynamic response*

The dynamic response of the inclined CNTRC sandwich beam under the moving mass is investigated in this sub-section. In Table 4, the DMFs of the sandwich beam with an inclined angle $\beta = \pi/5$ are tabulated for $v = 50$ m/s, $\zeta = 1$ and various values of the agglomeration parameter ξ and the CNT volume fraction V_{CNT} as well as the layer thickness ratio. One can observe from the

Table 2. Convergence of the formulation in evaluating fundamental frequency parameters of a composite beam reinforced with randomly oriented CNTs for different boundary conditions

Boundary conditions	Present						Ref. [30]	Error (%)
	$ne = 10$	$ne = 12$	$ne = 14$	$ne = 16$	$ne = 18$	$ne = 20$		
CF	2.0573	2.0571	2.0570	2.0570	2.0570	2.0570	2.151246	4.58
SS	3.4432	3.4428	3.4426	3.4425	3.4424	3.4424	3.574603	3.84

Table 3. Convergence of the formulation in computing DMF of the sandwich beam reinforced agglomerated CNTs for $\beta = \pi/5$, $V_{\text{CNT}} = 0.1$, $\zeta = 1$ and $v = 20$ m/s

		$ne = 16$	$ne = 20$	$ne = 24$	$ne = 28$	$ne = 32$
(2-1-2)	$\xi = 0.2$	0.7292	0.7292	0.7292	0.7292	0.7292
	$\xi = 0.5$	0.6339	0.6341	0.6342	0.6342	0.6342
	$\xi = 1$	0.5685	0.5687	0.5687	0.5687	0.5687
(2-2-1)	$\xi = 0.2$	0.7448	0.7448	0.7448	0.7448	0.7448
	$\xi = 0.5$	0.6581	0.6583	0.6583	0.6584	0.6584
	$\xi = 1$	0.5975	0.5977	0.5977	0.5977	0.5977

table the important role of the agglomeration parameter ξ on the DMF. At the given value of the parameter ζ, the DMF decreases when increasing the parameter ξ, and the decrease is more significant when the beam associated with a large CNT volume fraction value of V_{CNT}. As expected, the increase of the CNT volume fraction V_{CNT} and the face thickness leads to a significant decrease in the DMF. The influence of the CNT volume fraction and the face thickness on the DMF, however is governed by the agglomeration parameters. Looking at (1-1-1) sandwich beam with $\xi = \zeta = 1$ (uniformly distributed or no agglomeration), one can see from Table 4 that the factor D_d decreases 71.45% when increasing the V_{CNT} from 0 to 0.3, while the corresponding value is just 17.09% for the sandwich beam with $\xi = 0.1, \zeta = 1$ (severe CNT agglomeration). Examining the table in more detail one can see that the dependence of the DMF D_d upon the layer thickness ratio is significantly influenced by the agglomeration as well. Thus, one can conclude from the table that the increase of the CNT volume fraction and the reinforced face thickness is the most effective only when the CNTs agglomeration does not occur.

In Figure 6, the relation between the DMF D_d with the moving mass velocity v of the (1-2-1) and (2-1-2) beams are depicted for $\beta = \pi/5$ and different CNT volume fractions and the layer thickness ratios. Various remarks can be drawn from Figure 6. The CNT reinforcement, even with a small amount of CNT volume fraction of 0.02 can reduce the DMF significantly. However, the increase in the amount of reinforced CNTs is highly dependent on the CNTs agglomeration, regardless of the layer thickness ratio. For the case of severe agglomeration, that is when the two agglomeration parameters are far from each other such as $\xi = 0.1$, $\zeta = 1$ in Figure 6a,c, the DMF does not decrease considerably when increasing the CNT volume fraction V_{CNT}, and this tendency is more clearly for the beam associated with a larger V_{CNT}. In contrast, in case of no agglomeration, that is $\xi = \zeta = 1$ in Figure 6b,d, the increase of the CNT volume fraction leads to a sharp decrease in the DMF. By comparing Figure 6b with Figure 6d, one can see that the effect of the layer thickness ratio on the DMF is really evident only for the case of no CNT agglomeration. The dependence of the DMF upon the moving mass velocity is similar to that of the FGM beams subjected a moving load [31], and the DMF repeatedly increases and decreases when increasing the moving mass velocity v, and it then approaches a maximum value. The moving mass velocity

Table 4. DMFs of sandwich beam with $\beta = \pi/5$ for $v = 50$ m/s, $\zeta = 1$ and different values of agglomeration parameter ξ and CNT volume fraction

	$\zeta = 1$	$V_{CNT} = 0$	$V_{CNT} = 0.02$	$V_{CNT} = 0.05$	$V_{CNT} = 0.1$	$V_{CNT} = 0.2$	$V_{CNT} = 0.3$
	$\xi = 0.1$	1.4320	1.3066	1.2453	1.2096	1.1880	1.1815
(1-0-1)	$\xi = 0.5$	1.4320	1.2460	1.0677	0.8970	0.7337	0.6560
	$\xi = 1$	1.4320	1.2341	1.0189	0.7839	0.5289	0.3955
	$\xi = 0.1$	1.4320	1.3077	1.2466	1.2110	1.1889	1.1819
(2-1-2)	$\xi = 0.5$	1.4320	1.2476	1.0703	0.9001	0.7369	0.6589
	$\xi = 1$	1.4320	1.2358	1.0218	0.7875	0.5323	0.3982
	$\xi = 0.1$	1.4320	1.3111	1.2515	1.2165	1.1945	1.1873
(1-1-1)	$\xi = 0.5$	1.4320	1.2525	1.0787	0.9109	0.7486	0.6705
	$\xi = 1$	1.4320	1.2409	1.0310	0.7992	0.5442	0.4088
	$\xi = 0.1$	1.4320	1.3205	1.2652	1.2326	1.2120	1.2052
(2-2-1)	$\xi = 0.5$	1.4320	1.2662	1.1033	0.9436	0.7864	0.7096
	$\xi = 1$	1.4320	1.2554	1.0582	0.8360	0.5842	0.4465
	$\xi = 0.1$	1.4320	1.3214	1.2662	1.2335	1.2127	1.2056
(1-2-1)	$\xi = 0.5$	1.4320	1.2673	1.1044	0.9440	0.7856	0.7080
	$\xi = 1$	1.4320	1.2565	1.0592	0.8357	0.5820	0.4433
	$\xi = 0.1$	1.4320	1.3417	1.2958	1.2681	1.2502	1.2440
(1-4-1)	$\xi = 0.5$	1.4320	1.2967	1.1575	1.0143	0.8670	0.7918
	$\xi = 1$	1.4320	1.2878	1.1177	0.9147	0.6678	0.5244

at which the DMF attains the maximum value is higher for the sandwich beam reinforced with a higher CNT volume fraction, and this tendency is more visible for the beam with a larger face layer thickness and no CNT agglomeration in the beam (Figure 6d).

The effect of the inclined angle on the dynamic response of the CNTRC sandwich beam is shown in Figure 7, where the relation between the DMF with the moving mass velocity of the (2-1-2) beam is depicted for $V_{CNT} = 0.1$ and different agglomeration parameters. A significant decrease of the DMF by increasing the inclined angle is seen from the figure, regardless of the agglomeration parameters and the moving mass velocity. The influence of the inclined angle on the dynamic response is more significant for the case of CNT agglomeration (Figure 7a) than for the case of full dispersion (Figure 7b). Looking closely at Figure 7 one can see that although the inclined angle can significantly change the DMF, the angle hardly alter the shape of the curves in the figure as well as the velocity value at which the DMF attains the maximum value. The figure also confirms again the above remark on the influence of the CNT agglomeration, namely the DMF obtained for the beam without CNT agglomeration (Figure 7b) is considerably lower than that of the beam with severe CNT agglomeration (Figure 7a).

The influence of the two agglomeration parameters on the dynamic response of the sandwich beam is shown in Figure 8, where the variation of the DMF with the first agglomeration parameter ξ of the (2-1-2) beam is depicted for $\beta = \pi/5$, $V_{CNT} = 0.1$ and various values of agglomeration parameter ζ. For $\xi < \zeta$, the DMF decreases with an increase of the parameter ξ, and it attains the lowest value when $\xi = \zeta$, which corresponds to the case of uniform distribution of CNTs. For $\xi > \zeta$, the agglomeration degree is more serious when ξ is far from ζ, and the DMF increases again when increasing the parameter ξ. One can see from Figure 8 that the larger difference between the two agglomeration parameters is the higher DMF the beam has. Thus, the DMF is clearly underestimated by ignoring the agglomeration of CNTs.

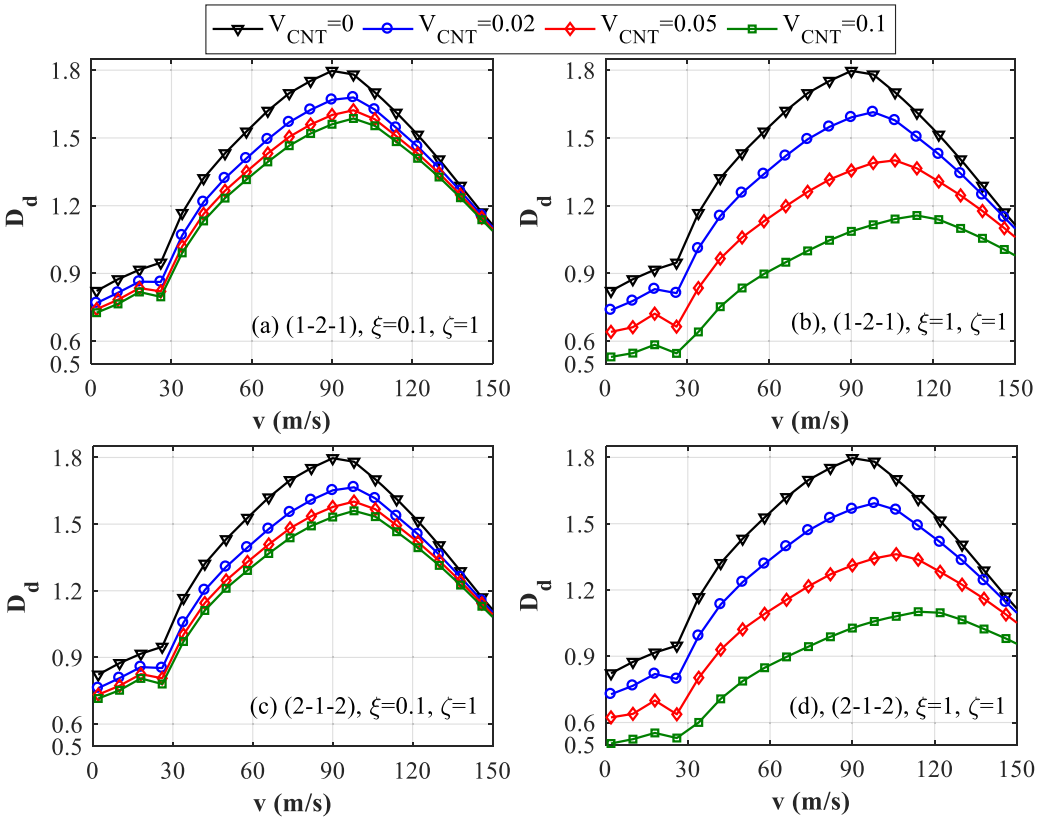

Figure 6. Relation between DMF with moving mass velocity of sandwich beam for $\beta = \pi/5$ and different CNT volume fractions and layer thickness ratios.

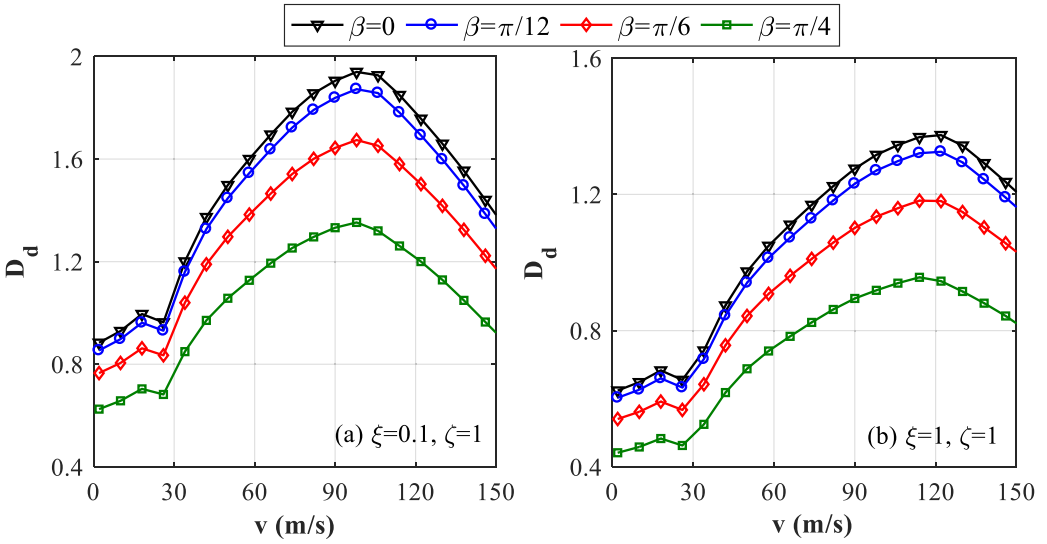

Figure 7. The effect of inclined angle on the relation between the DMF and moving mass velocity of (2-1-2) beam with $V_{\mathrm{CNT}} = 0.1$ and different agglomeration parameters.

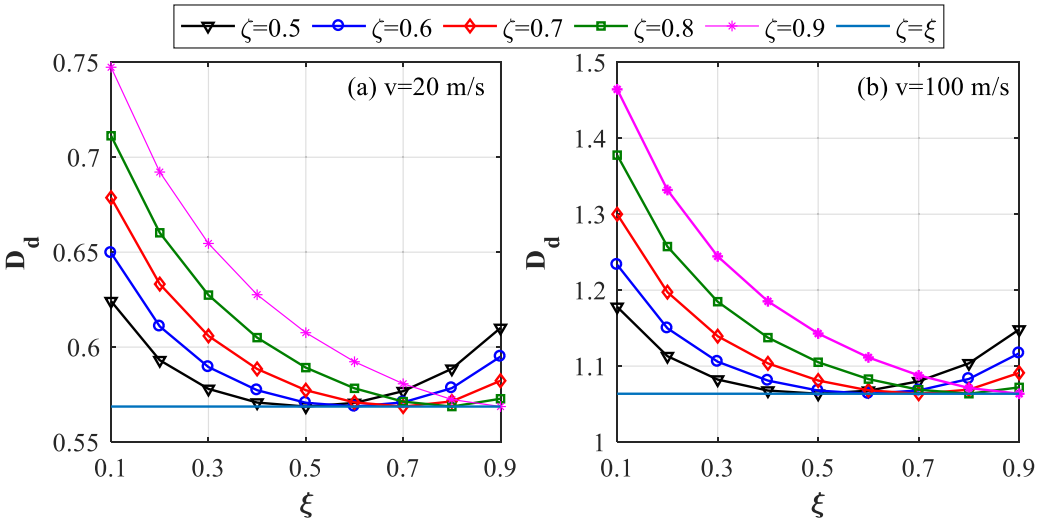

Figure 8. Variation of DMF with agglomeration parameter ξ of (2-1-2) beam with $\beta = \pi/5$, $V_{\mathrm{CNT}} = 0.1$ and various values of agglomeration parameter ζ.

It would be remiss not to consider the influence of the agglomeration on the time history of the inclined sandwich beam. Figure 9 displays the time histories for mid-span deflection of (2-1-2) sandwich beam for $\beta = \pi/5$, $V_{\mathrm{CNT}} = 0.1$, $\xi = 1$ and various values of the agglomeration parameters. It can be seen from the figure that the mid-span deflection of the beam reaches the smallest value when $\zeta = \xi = 1$, and it attains the maximum value when the two agglomeration parameters are farthest apart, regardless of the moving mass velocity. In addition, the beam tends to execute less vibration cycles when it is subjected to the mass moving with a higher velocity. The time at which the deflection reaches its maximum value is earlier as the two parameters closer to each other. In addition, it seems that the change of the second agglomeration parameter ζ has a stronger effect on the mid-span deflection of the beam, and this can be confirmed by comparing Figure 9b,d with Figure 9a,c.

6. Conclusions

The dynamics of the inclined sandwich beams with agglomerated carbon nanotube reinforced face sheets under a moving mass has been studied in the basis of the trigonometric shear deformation theory. The Mori–Tanaka approach, taking into consideration of CNT agglomeration is employed to estimate the material properties of the CNTRC layers. A novel finite element formulation in which the transverse shear rotation is employed as an independent variable is derived and used to establish the discretized equation of motion for the sandwich beams. Dynamic characteristics, including the dynamic magnification factors and the time histories for mid-span deflections are obtained for a simply supported sandwich beam with the aid of Newmark method. The effects of the inclined angle, the CNT agglomeration, the mass velocity as well as the layer thickness ratio on the dynamic response have been investigated in detail. The present study yields the following main conclusions:

(1) The CNT reinforcement significantly improves the dynamic response of the inclined sandwich beams. An increase in the CNTs volume fraction leads to a sharp decrease in the dynamic magnification factor, especially for the beam with a low degree of the CNT agglomeration.

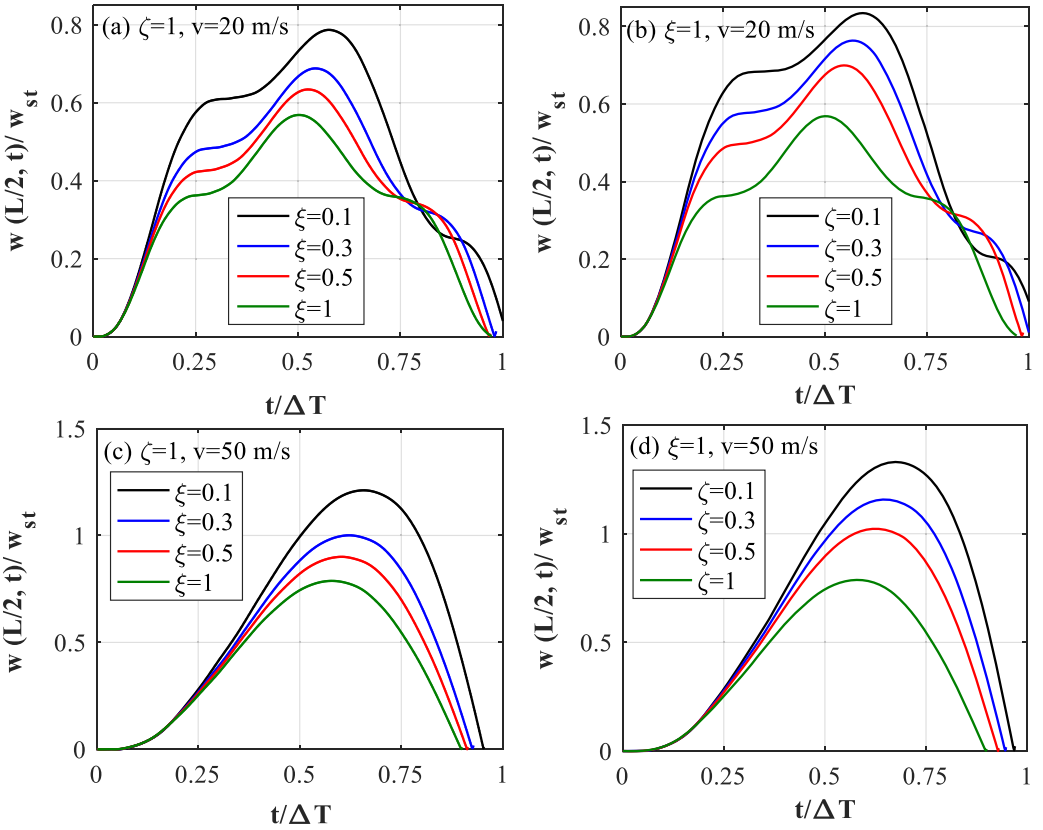

Figure 9. Time histories for mid-span deflection of (2-1-2) beam for $\beta = \pi/5$ and various values of two agglomeration parameters.

(2) CNT agglomeration has an impact role in dynamic response of the sandwich composite beams. The more severe agglomeration of the CNTs is, the higher dynamic magnification factor the beam has.
(3) The inclined angle plays an important role on the dynamic response of the sandwich composite beams, and the dynamic magnification factors of the beams are sharply decreased by increasing the inclined angle.
(4) The layer thickness ratio has a pronounced effect on the dynamic behavior of the sandwich beam. An increase of the CNT reinforced surface layer thickness leads to a significant decrease in the dynamic magnification factor, but this reduction is highly dependent on the CNTs volume fraction and the CNT agglomeration.

Declaration of interests

The authors do not work for, advise, own shares in, or receive funds from any organization that could benefit from this article, and have declared no affiliations other than their research organizations.

Acknowledgement

This research was made possible by the grant number CSCL03.02/22-23, Institute of Mechanics, VAST (Vietnam).

References

[1] S. Iijima, "Helical microtubules of graphitic carbon", *Nature* **354** (1991), p. 56-58.

[2] L. L. Ke, J. Yang, S. Kitipornchai, "Nonlinear free vibration of functionally graded carbon nanotubereinforced composite beams", *Compos. Struct.* **92** (2010), no. 3, p. 676-683.

[3] L. L. Ke, J. Yang, S. Kitipornchai, "Dynamic stability of functionally graded carbon nanotube reinforced composite beams", *Mech. Adv. Mater. Struct.* **20** (2013), no. 1, p. 28-37.

[4] M. H. Yas, N. Samadi, "Free vibrations and buckling analysis of carbon nanotube reinforced composite Timoshenko beams on elastic foundation", *Int. J. Pressure Vessels Pip.* **98** (2012), p. 119-128.

[5] H.-S. Shen, Y. Xiang, "Nonlinear analysis of nanotube-reinforced composite beams resting on elastic foundations in thermal environments", *Eng. Struct.* **56** (2013), p. 698-708.

[6] R. Ansari, M. Faghih Shojaei, V. Mohammadi, R. Gholami, F. Sadeghi, "Nonlinear forced vibration analysis of functionally graded carbon nanotube-reinforced composite Timoshenko beams", *Compos. Struct.* **113** (2014), p. 316-327.

[7] F. Lin, Y. Xiang, "Vibration of carbon nanotube reinforced composite beams based on the first and third order beam theories", *Appl. Math. Model.* **38** (2014), no. 15–16, p. 3741-3754.

[8] H. L. Wu, S. Kitipornchai, "Free vibration and buckling analysis of sandwich beams with functionally graded carbon nanotube-reinforced composite face sheets", *Int. J. Struct. Stab. Dyn.* **15** (2015), no. 7, article no. 1540011.

[9] H. L. Wu, J. Yang, S. Kitipornchai, "Nonlinear vibration of functionally graded carbon nanotube-reinforced composite beams with geometric imperfections", *Compos. Part B: Eng.* **90** (2016), p. 86-96.

[10] F. Ebrahimi, N. Farazmandnia, "Thermo-mechanical vibration analysis of sandwich beams with functionally graded carbon nanotube-reinforced composite face sheets based on a higher-order shear deformation beam theory", *Mech. Adv. Mater. Struct.* **24** (2017), no. 10, p. 820-829.

[11] A. Mohseni, M. Shakouri, "Vibration and stability analysis of functionally graded CNT-reinforced composite beams with variable thickness on elastic foundation", *Proc. Inst. Mech. Eng. L* **233** (2019), no. 12, p. 2478-2489.

[12] Ö. Civalek, Ş. D. Akbaş, B. Akgöz, S. Dastjerdi, "Forced vibration analysis of composite beams reinforced by carbon nanotubes", *Nanomaterials* **11** (2021), no. 3, p. 571-586.

[13] R. I. Rubel, M. H. Ali, M. A. Jafor, M. M. Alam, "Carbon nanotubes agglomeration in reinforced composites: a review", *AIMS Mater. Sci.* **6** (2019), no. 5, p. 756-780.

[14] D. L. Shi, X. Q. Feng, Y. Y. Huang, K. C. Hwang, H. Gao, "The effect of nanotube waviness and agglomeration on the elastic property of carbon nanotube reinforced composites", *J. Eng. Mater. Technol.* **126** (2004), no. 3, p. 250-257.

[15] M. Heshmati, M. H. Yas, "Free vibration analysis of functionally graded CNT-reinforced nanocomposite beam using Eshelby–Mori–Tanaka approach", *J. Mech. Sci. Technol.* **27** (2013), p. 3403-3408.

[16] M. Nejati, M. M. Najafizadehand, A. Eslampanah, "Buckling and vibration analysis of functionally graded carbon nanotube-reinforced beam under axial load", *Int. J. Appl. Mech.* **8** (2016), no. 1, article no. 1650008.

[17] S. Kamarian, M. Shakeri, M. H. Yas, M. Bodaghi, A. Pourasghar, "Free vibration analysis of functionally graded nanocomposite sandwich beams resting on Pasternak foundation by considering the agglomeration effect of CNTs", *J. Sandwich Struct. Mater.* **17** (2015), no. 6, p. 632-665.

[18] S. Kamarian, M. Bodaghi, A. Pourasghar, S. Talebi, "Vibrational behavior of non-uniform piezoelectric sandwich beams made of CNT-reinforced polymer nanocomposite by considering the agglomeration effect of CNTs", *Polym. Compos.* **38** (2017), no. S1, p. E553-E562.

[19] J. Pan, L. Bian, "Influence of agglomeration parameters on carbon nanotube composites", *Acta Mech.* **228** (2017), p. 2207-2217.

[20] F. Kiani, Y. Ariaseresht, A. Niroumand, H. Afshari, "Thermo-mechanical buckling analysis of thick beams reinforced with agglomerated CNTs with temperature-dependent thermo-mechanical properties under a nonuniform thermal loading", *Mech. Des. Struct. Mach.* (2022).

[21] X. G. Yue, S. Sahmani, H. Luo, B. Safaei, "Nonlocal strain gradient-based quasi-3D nonlinear dynamical stability behavior of agglomerated nanocomposite microbeams", *Archiv. Civ. Mech. Eng.* **23** (2023), no. 1, article no. 21.

[22] J. J. Wu, "Dynamic analysis of an inclined beam due to moving loads", *J. Sound Vib.* **288** (2005), no. 1–2, p. 107-131.

[23] E. Bahmyari, S. R. Mohebpour, P. Malekzadeh, "Vibration analysis of inclined laminated composite beams under moving distributed masses", *Shock Vib.* **2014** (2014), article no. 750916.

[24] A. Mamandi, M. H. Kargarnovin, D. Younesian, "Nonlinear dynamics of an inclined beam subjected to a moving load", *Nonlinear Dynam.* **60** (2010), p. 277-293.

[25] A. Mamandi, M. H. Kargarnovin, "Dynamic analysis of an inclined Timoshenko beam traveled by successive moving masses/forces with inclusion of geometric nonlinearities", *Acta Mech.* **218** (2011), p. 9-29.

[26] D. K. Nguyen, T. T. Tran, V. N. Pham, T. N. A. Le, "Dynamic analysis of an inclined sandwich beam with bidirectional functionally graded face sheets under a moving mass", *Eur. J. Mech. A/Solids* **88** (2021), article no. 104276.

[27] J. R. Zuiker, "Functionally graded materials: choice of micromechanics model and limitations in property variation", *Compos. Eng.* **5** (1995), no. 7, p. 807-819.

[28] H. Daghigh, V. Daghigh, "Free vibration of size and temperature-dependent carbon nanotube (CNT)-reinforced composite nanoplates with CNT agglomeration", *Polym. Compos.* **40** (2019), no. S2, p. E1479-E1494.
[29] A. J. M. Ferreira, C. M. C. Roque, R. M. N. Jorge, "Analysis of composite plates by trigonometric shear deformation theory and multiquadrics", *Comput. Struct.* **83** (2005), p. 2225-2237.
[30] M. H. Yas, M. Heshmati, "Dynamic analysis of functionally graded nanocomposite beams reinforced by randomly oriented carbon nanotube under the action of moving load", *Appl. Math. Model.* **36** (2012), p. 1371-1394.
[31] M. Şimşek, "Vibration analysis of a functionally graded beam under a moving mass by using different beam theories", *Compos. Struct.* **92** (2010), p. 904-917.